JOURNAL OF SOLID STATE CHEMISTRY 54, 426–437 (1984)

A Study of the $Li_{1+x}Ti_{2-x}O_4$ Spinel System by Diffuse-Reflectance Spectroscopy*

M. R. HARRISON,† P. P. EDWARDS,†‡, AND J. B. GOODENOUGH

Inorganic Chemistry Laboratory, Oxford University, South Parks Road, Oxford OX1 3QR, United Kingdom

Received February 10, 1984

The room-temperature diffuse-reflectance spectra of compositions within the $Li_{1+x}Ti_{2-x}O_4$ spinel system ($0 \leq x \leq \frac{1}{3}$) show three absorption bands in the range 4000 to 48,000 cm^{-1}. Two high-energy absorption bands correspond to charge-transfer transitions from the oxygen-2*p* valence band to the titanium t_{2g} and σ^* conduction bands, where the σ^* band of e_g character has hybridized titanium-3*d* and titanium-4*s* parentage. The absorption band arising from promotion of electrons to the empty σ^* band does not alter with composition whereas the absorption band arising from promotion of electrons to the partially filled t_{2g} band narrows as the concentration of conduction electrons in the t_{2g} band decreases. These two high-energy absorption bands fall entirely within the ultraviolet spectral region, and the absorption edge in $Li_{4/3}Ti_{5/3}O_4$ ($x = \frac{1}{3}$) occurs at 24,300 cm^{-1} (3.02 eV). A low-energy absorption band is observed in compositions with $x < \frac{1}{3}$ and in samples of $Li_{4/3}Ti_{5/3}O_4$ reduced in hydrogen at elevated temperatures. This band straddles the boundary between the visible and infrared spectral regions and shifts toward lower energy as the concentration of conduction electrons in the t_{2g} band decreases. The possible origins of the band are discussed; the argument is in favor of a *d–d* interband transition from states in the partially filled t_{2g} band to states in the empty σ^* band.

Introduction

The spinel system $Li_{1+x}Ti_{2-x}O_4$ ($0 \leq x \leq \frac{1}{3}$) (*1*) has attracted much attention following the discovery by Johnston *et al.* (*2–6*) of high-temperature superconductivity ($T_c \simeq 11$ K) in the compositional range $0 \leq x \leq 0.1$. The disappearance of the superconductivity at $x = 0.1$ pointed to a metal–insulator transition (MIT) at that composition, but the nature of this MIT was not resolved in the subsequent work on this system (*7–13*). We have studied the $Li_{1+x}Ti_{2-x}O_4$ spinel system in detail (*14*), and we have presented magnetic susceptibility, electron-spin resonance (ESR) spectroscopy, and photoelectron (PE) spectroscopy measurements on these materials (*15, 16*). In this paper, we present diffuse-reflectance spectroscopy measurements on the same samples.

The spinel structure is shown in Fig. 1. The tetrahedral sites in $Li_{1+x}Ti_{2-x}O_4$ are occupied entirely by lithium ions whereas the

* Dedicated to Dr. M. J. Sienko.

† Present address: University Chemical Laboratory, Cambridge University, Lensfield Road, Cambridge CB2 1EW, United Kingdom.

‡ To whom correspondence should be addressed.

0022-4596/84 $3.00

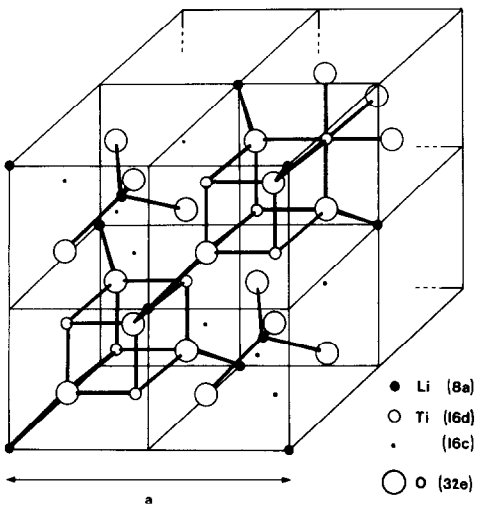

FIG. 1. The spinel structure of $LiTi_2O_4$ ($x = 0$) showing the tetrahedral sites (8a), octahedral sites (16d), and unoccupied interstitial octahedral sites (16c). The origin of the unit cell is taken as a tetrahedral site in this figure, and the site labels are taken from Ref. (*33*).

octahedral sites are randomly occupied by (x) lithium ions and ($2 - x$) titanium ions per formula unit. Each titanium ion resides at the center of a trigonally distorted octahedron of oxygen ions, and the titanium-3*d* states are split by the cubic component of the crystal field into more stable t_{2g} and less stable e_g states. The octahedra share edges with each other, and the titanium–titanium separation through the edges of the octahedra remains below 3 Å over the entire compositional range $0 \leq x \leq \frac{1}{3}$ (*15*). Direct titanium–titanium interactions are therefore responsible for the formation of a t_{2g} conduction band (*17*) that is broader than the splitting of the t_{2g} states due to the trigonal component of the crystal field (*16*). The bottom of this band lies ~3 eV above the top of the oxygen-2*p* valence band.

The resulting band structure is shown in Fig. 2. The partial occupation of the octahedral sites by lithium ions changes the number of electrons in the t_{2g} conduction band, and the Fermi energy, E_F, moves toward the bottom of the band as the lithium fraction increases. The band is one-twelfth full in metallic $LiTi_2O_4$ ($x = 0$) and empty in insulating $Li_{4/3}Ti_{5/3}O_4$ ($x = \frac{1}{3}$). PE spectra of these materials were compatible with the band structure shown in Fig. 2, and the spectrum of $LiTi_2O_4$ showed a distinct t_{2g} conduction band that terminated in a sharp Fermi edge. However, the detailed shape of the band together with the superconducting properties of this material led us to postulate a strong interaction of the conduction electrons with the lattice vibrations. The corresponding optical properties of the conduction electrons perturbed by this interaction are therefore of interest.

The partial occupation of the octahedral sites by lithium ions perturbs the t_{2g} conduction band in addition to reducing the number of conduction electrons in this band. A random distribution of lithium ions will result in the introduction of a mobility edge, E_c, separating localized ($E_c > E$) and itinerant ($E > E_c$) electron states as shown in Fig. 2 (*18*). E_c increases in energy and E_F

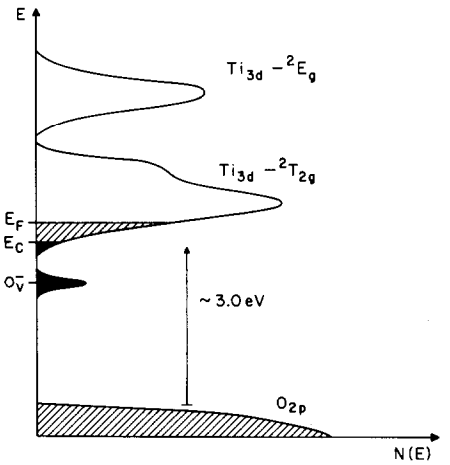

FIG. 2. The band structure of a metallic sample of $Li_{1+x}Ti_{2-x}O_4$ with a low value of x. Lightly shaded states in the titanium-3d bands are occupied by itinerant electrons; heavily shaded states by localized electrons. States labeled O_V^- arise from electrons trapped at oxygen vacancies (see text for details).

decreases in energy as the lithium fraction increases, and an Anderson MIT would occur at the composition where E_c is equal to E_F (*18*).

The results obtained on this system by Johnston *et al.* (*2–6*) were consistent with the occurrence of an Anderson MIT at $x = 0.1$, and the nature of the localized states below E_c is of particular interest. The wavefunctions of these localized states are centered at individual titanium sites in the crystal, and the envelope of the wavefunctions decreases exponentially with distance from the titanium sites (*18*). This exponential decay of the envelope defines a localization length for the wavefunctions of the localized states. For states slightly below E_c, the localization length will be very large and the wavefunctions will encompass the bulk of the titanium ions in the crystal. For states considerably below E_c at the bottom of the t_{2g} band, the localization length will be very small and the wavefunctions will only encompass the neighboring titanium ions. The optical properties of these strongly localized states at the bottom of the t_{2g} band are expected to be different from the properties of the extended states above E_c.

ESR spectra (*15*) have indicated the presence of two types of localized states in this system, both comprising electrons trapped at defects in the lattice. In both cases, an unpaired electron was trapped as a Ti^{3+} ion in a crystal field that was predominantly octahedral, but with a strong tetragonal component. This type of crystal field cannot arise in the stoichiometric spinel, and we proposed two types of defect: an oxygen vacancy and a hydroxyl ion. Unpaired electrons are trapped as Ti^{3+} ions adjacent to these defects, and the strong tetragonal field is associated with the formation of a static $(TiO)^+$ ion by a displacement of the titanium ion from the defect. The signals from the trapped electrons broaden with increasing temperature and then disappear when the static displacement of the $(TiO)^+$ ion starts to break down. In the case of electrons trapped by oxygen vacancies, the breakdown occurs above room temperature. In the case of electrons trapped by hydroxyl ions, however, the breakdown occurs at a temperature which depends upon the concentration of electrons in the t_{2g} conduction band and the perturbation of this band by lithium ions or by defects.

In samples of $Li_{1+x}Ti_{2-x}O_4$ with $x < \frac{1}{3}$, the signal from electrons trapped by oxygen vacancies was visible in samples over the entire compositional range. In contrast, the signal from electrons trapped at hydroxyl ions was detectable to ~30 K only in those samples with $x \geq 0.2$. Thus the hydroxyl ions in these samples trap electrons at comparatively low temperatures. In samples of $Li_{4/3}Ti_{5/3}O_4$ ($x = \frac{1}{3}$) reduced in hydrogen at elevated temperatures, a signal from electrons trapped by oxygen vacancies was visible only in samples that had been heavily reduced (labeled H) (*15*). In contrast, a signal from electrons trapped by hydroxyl ions was detectable almost to room-temperature even in those samples that had been lightly reduced (labeled L) (*15*). Thus the hydroxyl ions in these samples trap electrons to comparatively high temperatures. The optical properties of the conduction electrons trapped by these defects are therefore of particular interest. To investigate these points, we chose to study the room-temperature diffuse-reflectance spectra of compositions within the homogeneity range $0 \leq x \leq \frac{1}{3}$.

Experimental Methods

Powder samples of $Li_{1+x}Ti_{2-x}O_4$ ($0 \leq x \leq \frac{1}{3}$) were prepared by heating together stoichiometric quantities of Li_2TiO_3, Ti_2O_3 (Ventron Alfa, 99%), and TiO_2 (Ventron Alfa, 99.8%) at 800°C either under a dynamic vacuum ($x < \frac{1}{3}$) or in oxygen ($x = \frac{1}{3}$) as previously described (*15*). The Li_2TiO_3

was itself prepared by heating together stoichiometric quantities of Li_2CO_3 (BDH Analar Grade) and TiO_2 at 800°C in oxygen. The samples were characterized by X-ray powder-diffraction measurements (*15*). Examination of the powders under an electron microscope indicated a uniform particle size of ~5 μm.

Diffuse-reflectance spectra were recorded at room temperature in the range 4000 to 48,000 cm^{-1} (approximately 0.5 to 6.0 eV) with a Unicam SP700 spectrometer equipped with an SP735 diffuse-reflectance attachment. The sample holder in this attachment was divided into two halves: one half contained the pure sample; the other half contained the MgO reference material. The section of the transparent cover over the reference material was freshly coated with finely powdered MgO produced by burning pieces of magnesium ribbon.

The reflected radiation measured in a diffuse-reflectance experiment generally contains both a diffuse component and a specular component. The diffuse component consists of the radiation reflected isotropically from the sample surface after repeated scattering from the surfaces of the particles. It has been demonstrated (*19*) that the variation with frequency of the diffuse component is very similar to the variation with frequency of the intensity transmitted through a crystal of the material (i.e., an absorbance spectrum). The specular component consists of the radiation reflected normally to the sample surface (i.e., a reflectance spectrum).

The positions of any absorption bands may be obtained with high accuracy in a diffuse-reflectance experiment, although the intensities of the bands are of lesser significance (*19*). The relative contributions of the diffuse and specular components depend upon the nature of the sample. For example, if the plasma resonance of a metallic material falls within the spectral range of the spectrometer, the sample will be strongly reflecting below the plasma frequency and weakly reflecting above the plasma frequency (*20, 21*). The strong specular component arising from the plasma resonance will then dominate the diffuse component arising from interband transitions. Since some of the $Li_{1+x}Ti_{2-x}O_4$ samples examined in this work are metallic, it is important to distinguish the specular and diffuse components in this material. Fortunately, Dickens *et al.* (*22*) have made diffuse-reflectance measurements on powder samples of the sodium tungsten bronzes Na_xWO_3 using the spectrometer described above; they have shown that the specular component may be reduced by diluting the samples with an excess of the reference material. The optical properties of the sodium tungsten bronzes are well known from measurements on crystals (*23, 24*), and it is of interest to compare the spectra obtained by the different techniques.

Measurements on metallic crystals fit extremely well to the classical Drude free-electron model (*20, 21*) at low energy if the effective mass of the conduction electrons is permitted to increase with increasing sodium content (*23, 24*). At high energy, the spectra show the charge-transfer transitions from the oxygen-2*p* valence band to the tungsten-5*d* conduction bands. However, at lower energy the expected interband transitions within the tungsten-*d* conduction bands are obscured by the plasma resonance.

Diffuse-reflectance measurements on *undiluted* metallic powders showed a single absorption feature, and Dickens *et al.* (*22*) attributed this peak to a minimum in the reflectance of the samples associated with a plasma resonance of the conduction electrons. Owen *et al.* (*23*) were subsequently able to show that the energy of the peak could be quantitatively related to the plasma frequency obtained from crystal spectra. Thus the diffuse-reflectance spectra of undiluted metallic powders were

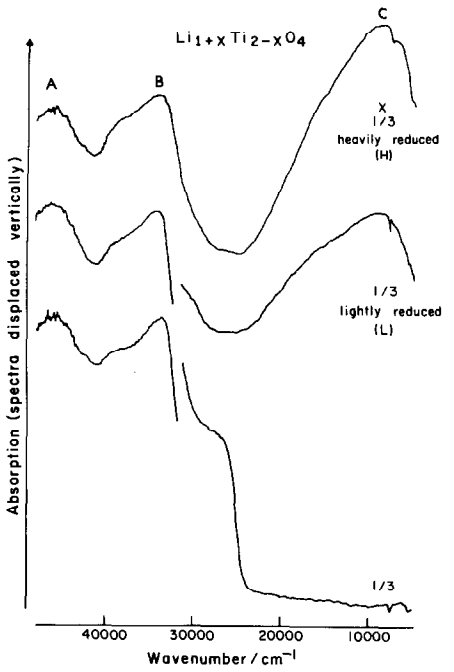

FIG. 3. Room-temperature diffuse-reflectance spectra of samples of $Li_{4/3}Ti_{5/3}O_4$ ($x = \frac{1}{3}$) unreduced, lightly reduced (L) and heavily reduced (H) in hydrogen at elevated temperatures. The three absorption bands are labeled A, B, and C. The sudden break in the curves indicates a change from the higher to the lower absorbance range of the spectrometer in the low-energy region of the spectra.

dominated by the specular-reflectance component. In contrast, diffuse-reflectance measurements on *diluted* metallic powders showed two absorption features. Dickens *et al.* (*22*) attributed the high-energy peak to the charge-transfer transitions between the oxygen-2*p* valence band and the tungsten-5*d* conduction bands, and the low-energy peak to interband transitions within the tungsten-5*d* conduction bands. Thus the diffuse reflectance spectra of the diluted metallic samples are dominated by the diffuse-reflectance component and reveal the underlying interband transitions.

Results

The room-temperature diffuse-reflectance spectra of all the powdered samples are shown in Figs. 3 and 4. Three absorption bands are generally observed in the range 4000 to 48,000 cm^{-1}; they are labeled A, B, and C for convenience. All of the spectra were obtained from undiluted samples. Dilution of the samples with a large excess of the reference material MgO had no significant effect on the spectra apart from reducing the peak intensities. In the case of the blue, vacuum-fired samples with $x < \frac{1}{3}$, the variation of the spectra with composition is continuous; there is no evidence of any discontinuities in either the peak positions or peak intensities of these bands at any composition. In the case of the blue, hydrogen-reduced samples with $x = \frac{1}{3}$, there is no evidence of any discontinuities in either the peak positions or peak in-

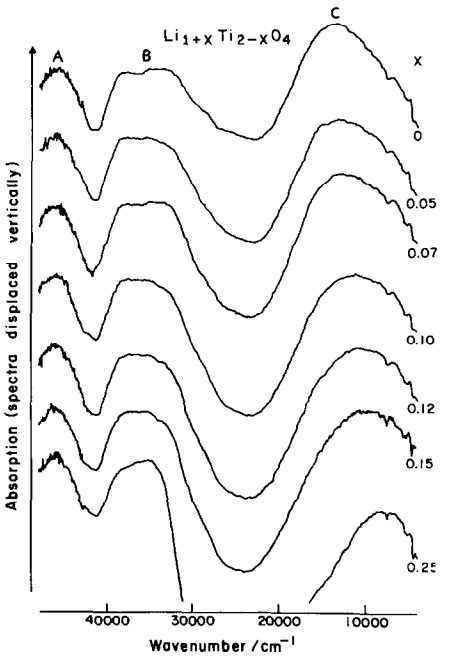

FIG. 4. Room-temperature diffuse-reflectance spectra of samples of $Li_{1+x}Ti_{2-x}O_4$ ($x < \frac{1}{3}$). The three absorption bands are labeled A, B, and C.

tensities of these bands with the degree of reduction.

Only two of these absorption bands (A and B) are visible in the spectrum of white, unreduced $Li_{4/3}Ti_{5/3}O_4$ ($x = \frac{1}{3}$) (Fig. 3), the region below 20,000 cm^{-1} being featureless. A strong absorption edge occurs on the low-energy side of band B, and the position of this edge is measured to be 24,300 cm^{-1} (3.02 eV), which is well within the ultraviolet spectral region. A similar strong absorption edge (3.03 eV) is observed in the spectrum of unreduced TiO_2 (rutile) (*25*). Referring to Fig. 2, we anticipate that bands A and B correspond to strong charge-transfer transitions from the oxygen-2*p* valence band to the titanium t_{2g} and σ^* conduction bands, where the σ^* band of e_g character has hybridized titanium-3*d* and titanium-4*s* parentage. These measurements therefore determine the magnitude of the energy gap between the valence and conduction bands in $Li_{4/3}Ti_{5/3}O_4$ to be 3.02 eV.

The band A arising from promotion of electrons to the empty σ^* energy band does not appear to alter with composition in the vacuum-fired samples with $x < \frac{1}{3}$ or with the degree of reduction in the hydrogen-reduced samples with $x = \frac{1}{3}$. In contrast, the band B involving promotion of electrons to the partially filled t_{2g} energy band appears to narrow as the lithium fraction of the vacuum-fired samples with $x < \frac{1}{3}$ increases. The band B does not alter with the degree of reduction in the hydrogen-reduced samples with $x = \frac{1}{3}$. The significance of this compositional dependence is considered in the Discussion section.

A third absorption band C is visible in the spectra of the blue, hydrogen-reduced samples of $Li_{4/3}Ti_{5/3}O_4$ ($x = \frac{1}{3}$) (Fig. 3). The peak *intensity* of this band varies strongly with the degree of reduction of the samples, and the peak intensity for sample H is much greater than the peak intensity for sample L. This is in accord with the variation in the color of the samples; sample H was dark blue while sample L was pale blue. In contrast, the peak *position* of this band does not vary noticeably with the degree of reduction of the sample and remains at 8900 cm^{-1}.

A similar color change arising from a low-energy absorption band occurs when samples of TiO_2 are reduced. This reduction can be achieved by heating the material in hydrogen or alkali-metal vapor at elevated temperatures (*26, 27*), or by implanting hydrogen or alkali-metal atoms by ion-bombardment techniques (*28, 29*). In either case, hydroxyl ions or alkali-metal ions are inserted into the lattice. These donor ions are able to trap electrons below a critical temperature; this temperature depends upon the concentration of electrons in the conduction band, the nature of the donor ions, and the perturbation of the conduction band caused by the donor ions or other defects created by the reduction. Above this critical temperature, the electrons introduced by the donor ions enter the conduction band.

Using this model we can explain the variation of the peak position and peak intensity of this band in different reduced samples of TiO_2. The peak *intensity* of the band varies strongly with the degree of reduction of the sample, and it is often used as a quantitative guide to the degree of reduction (*26, 27*). The peak *position* of the band may also vary with the degree of reduction of the sample, but the behavior is more complex. Generally, the peak position is found to be independent of both the measurement temperature and the nature of the donor ions, indicating that the electrons introduced by the donor ions enter the conduction band. The peak position then occurs at 6600 cm^{-1} (*26, 27*). However, low-temperature (<77 K) measurements on samples lightly reduced by hydrogen indicate a shift in this band to the higher energy of 9300

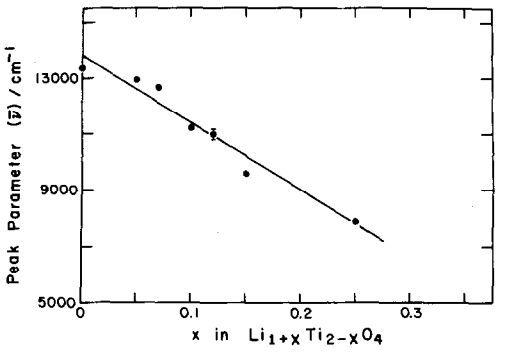

FIG. 5. Peak position, $\bar{\nu}$, of the low-energy absorption band C as a function of x in $Li_{1+x}Ti_{2-x}O_4$.

cm^{-1} (*30*), and the energy difference of ~2700 cm^{-1} (0.33 eV) may be attributed to the binding energy of an electron at a hydroxyl ion or possibly at an oxygen vacancy. This hypothesis is supported by room-temperature measurements on samples more heavily reduced in hydrogen, which indicate a similar band shift to higher energy (*31*), and by room-temperature measurements on samples heavily reduced by ion bombardment, which indicate a band shift to higher energy that depends upon the nature of the donor ions (*28, 29*).

By analogy from TiO_2 and from the presence of a high-temperature ESR signal from electrons trapped by hydroxyl ions and oxygen vacancies in the hydrogen-reduced samples of $Li_{4/3}Ti_{5/3}O_4$ ($x = \frac{1}{3}$), we conclude that the transition energy of 8900 cm^{-1} contains the binding energy of the excited electron to a hydroxyl ion or possibly to an oxygen vacancy.

The third absorption band C is also visible in the spectra of the blue, vacuum-fired samples with $x < \frac{1}{3}$ (Fig. 4). The peak *position* of this band changes significantly with the lithium fraction of the samples, varying between ~14,000 cm^{-1} where $x = 0$ and ~8000 cm^{-1} where $x = 0.25$. However, the peak *intensity* does not vary so strongly with the lithium fraction; the peak intensity of the band for the $x = 0$ sample being about twice as intense as the peak intensity of the band for the $x = 0.25$ sample. Thus the decrease observed in the depth of the blue color as the lithium fraction of the samples increases is due mostly to the shift in the peak position of the band toward the infrared spectral region rather than to a decrease in the peak intensity of the band.

Figure 5 shows the variation in the measured value of the peak position $\bar{\nu}$ of the band C with the nominal composition of the vacuum-fired samples ($x < \frac{1}{3}$). The error in the determination of the peak position is estimated as 200 cm^{-1}. The peak position varies approximately linearly with the composition parameter x with a least-square fit giving

$$\bar{\nu} = (-23{,}960x + 13{,}760)\ \text{cm}^{-1}, \quad (1)$$

and a correlation coefficient of 0.977.

We have previously shown that the lattice parameter of these vacuum-fired samples also varies linearly with the nominal composition of the samples (*15*). In fact, the deviation of the lattice-parameter values from the fitted line is very similar to the deviation of the peak-position values from the fitted line in Fig. 5, suggesting that the deviation is predominantly due to a variation of the composition of the samples from the nominal value. If this is indeed the case, we would expect a particularly strong correlation to occur between the lattice-parameter values and the peak-position values of the samples.

Figure 6 shows the variation in the estimated values of the peak position $\bar{\nu}$ of band C with the lattice parameter a. There is indeed a strong correlation between the two quantities, with a least-square fit giving

$$\bar{\nu} = (167{,}500a - 1{,}395{,}000)\ \text{cm}^{-1}, \quad (2)$$

and a correlation coefficient of 0.991. This correlation coefficient is significantly higher than the value of 0.977 obtained above. The significance of this correlation is considered in the Discussion section.

The lowest-energy peak position re-

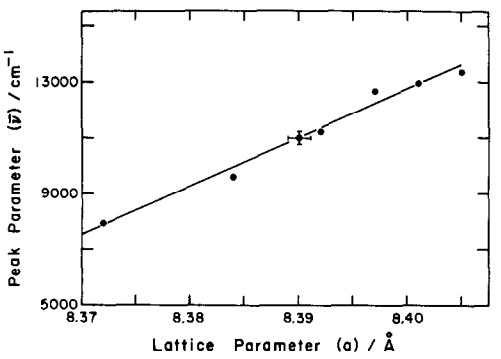

FIG. 6. Peak position, $\bar{\nu}$, of the low-energy absorption band C as a function of the lattice parameter, a, for samples of $Li_{1+x}Ti_{2-x}O_4$.

corded on Fig. 5 occurs at 7910 cm^{-1} for a sample with $x = 0.25$. Subsequent experimentation on samples with higher values of x approaching the phase limit have shown that the blue color persists, and a sample with a nominal composition of $x = 0.27$ was observed to have a peak position of 6500 cm^{-1}. The fitted line in Fig. 5 (Eq. (1)) extrapolates to a value of 5780 cm^{-1} at the phase limit. Unfortunately, it is difficult to prepare samples of precise composition in this compositional range since small variations in the sample-preparation conditions produce significant variations in the composition of the samples. The great majority of the conduction electrons in the t_{2g} band occur because of the nominal stoichiometry of the vacuum-fired samples; they are not introduced by reduction. This suggests that the transition energy of 5780 cm^{-1} does not contain the binding energy of the electron to a trap site; the excited electrons occupy states in the t_{2g} conduction band at room temperature.

We have shown that the properties of the low-energy absorption band C in the hydrogen-reduced samples of $Li_{4/3}Ti_{5/3}O_4$ ($x = \frac{1}{3}$) are very similar to those of the low-energy absorption band observed in hydrogen-reduced samples of TiO_2, and it is reasonable to assume a common mechanism for the transition in both materials. Unfortunately there is still no concensus on this mechanism in TiO_2, and several possible models have been advanced. In the Discussion section we consider each of these models in turn.

Discussion

Electrons Trapped by Defects

Both the oxygen-vacancy and hydroxyl-ion defects in $Li_{1+x}Ti_{2-x}O_4$ have been considered in detail in a previous paper (*15*). Both defects produce an imbalance in the Ti–O bonding that results in a titanium-ion displacement toward the oxygen ion on the opposite side of the octahedron. This displacement produces a strongly bonded Ti–O unit that is maintained on reduction of the Ti^{4+} ion to a Ti^{3+} ion, and the resulting Ti–O unit may be termed a $(TiO)^+$ "titanyl ion" by analogy to the $(VO)^{2+}$ vanadyl ion. The nature of the bonding within the vanadyl ion and the optical transitions that occur within it have been considered by Ballhausen and Gray (*32*). Besides the strong charge-transfer transitions, weak d–d interband transitions of the vanadyl ion are observed in the visible spectral range. It is conceivable that band C in $Li_{1+x}Ti_{2-x}O_4$ arises from a similar d–d interband transition of a titanyl ion associated with an oxygen vacancy or with a hydroxyl ion. Cronemayer (*31*) has suggested that the low-energy absorption band in hydrogen-reduced TiO_2 arises from electrons trapped by oxygen vacancies.

An electron trapped by an oxygen vacancy cannot alone be responsible for band C, however. The lightly reduced sample L exhibits band C at room temperature, but ESR measurements indicate that there are no oxygen vacancies in this sample (*15*). Moreover, the intensity of band C decreases monotonically with the lithium

fraction of the vacuum-fired samples with $x < \frac{1}{3}$. ESR measurements indicate that the concentration of oxygen vacancies in these samples depends upon the preparation conditions and generally varies randomly with the lithium fraction (*15*).

An electron trapped by a hydroxyl ion cannot alone be responsible for band C either. The lightly reduced sample L exhibits band C at room temperature, and ESR measurements suggest that the electron remains trapped by the hydroxyl ion to room temperature (*15*). The energy of band C in this sample is 8900 cm^{-1}. However, the vacuum-fired samples with $x < \frac{1}{3}$ all exhibit band C at room temperature, but ESR measurements show that the electron is only trapped by the hydroxyl ion in samples with high values of $x \geq 0.2$ below ~30 K (*15*). The energy of band C in these samples extrapolates to a value of 5780 cm^{-1} at the phase limit. We conclude that band C cannot arise from only *d–d* interband transitions within the titanyl ion, although the energy of this band is affected by the presence of the hydroxyl ions or possibly oxygen vacancies. Whatever the origin of band C, it occurs at a higher energy if the electrons are trapped; the additional energy of the transition reflects the binding energy of the electron at the defect. This binding energy is 3120 cm^{-1} (0.38 eV).

Plasma Resonance of Itinerant Electrons

The superconducting properties of Li Ti_2O_4 ($x = 0$) clearly indicate that the conduction electrons at the Fermi surface in this composition are itinerant. These electrons are expected to give rise to a characteristic maximum in the diffuse-reflectance spectrum associated with the plasma resonance of the conduction electrons. Dickens *et al.* (*22*) derived the following equation for the energy, in wavenumbers, of such a maximum in Na_xWO_3 as a function of the density of conduction electrons, n:

$$\bar{\nu} = \frac{1}{2\pi c}\sqrt{\frac{ne^2}{m^*\varepsilon_0(1+\varepsilon)}}. \qquad (3)$$

This equation is based on a Drude free-electron model (*20, 21*) that has been modified by the introduction of the dielectric constant of the lattice, ε, and the effective mass of the conduction electrons, m^*; ε_0 is the permittivity of the vacuum, e the charge of the electrons, and c the speed of light in a vacuum. Johnston (*4*) showed that the dielectric constant of $Li_{4/3}Ti_{5/3}O_4$ ($x = \frac{1}{3}$) was 11. Using this value in Eq. (3) and varying the value of m^*, we obtain good agreement with the peak position of band C for $m^*/m_0 = 0.55$, where m_0 is the mass of free electrons. This is shown in Fig. 7. Despite this good agreement, however, we do not believe that band C arises from a plasma-resonance mechanism. There is no change in the form of the diffuse-reflectance spectrum at the MIT, suggesting that we are observing an underlying interband spectrum. In addition, the absorption maximum associated with the plasma resonance should be suppressed by the dilution of the sample with the reference material to reveal the underlying interband spectrum (*22*), and this suppression was not observed. It is possible that the absorption maximum associated with the plasma resonance occurs outside

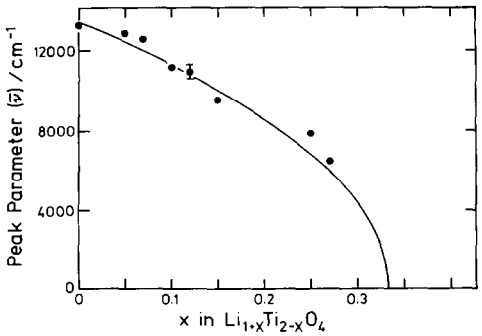

FIG. 7. Peak position, $\bar{\nu}$, of the low-energy absorption band C as a function of x in $Li_{1+x}Ti_{2-x}O_4$. The solid curve is Eq. (3) with the parameters $\varepsilon = 11$ and $m^*/m_0 = 0.55$.

the range of the spectrometer ($\bar{\nu} < 4000$ cm^{-1} corresponding to $m^*/m_0 > 6$); it is also possible that the postulated strong coupling of the conduction electrons with the lattice vibrations suppresses the absorption maximum (*20, 21*).

Hopping of Localized Polarons

As stated above, the superconducting properties of $LiTi_2O_4$ ($x = 0$) indicate that the conduction electrons at the Fermi surface in this composition are itinerant. However, the strong coupling of the conduction electrons with the lattice vibrations may be sufficient to form localized polaron states deeper in the t_{2g} conduction band that hop from site to site with an activation energy ~1 eV (~8000 cm^{-1}). This activation energy would then correspond to the energy of band C. Bogomolov *et al.* (*30*) have suggested that the low-energy absorption band in hydrogen-reduced TiO_2 arises from a polaron hopping mechanism. However, we do not believe that band C arises from such a mechanism since it is difficult to see why the hopping energy of the polaron should *decrease* with increasing lithium content in the vacuum-fired samples with $x < \frac{1}{3}$.

Excitation of t_{2g} Electrons to the σ^* Band

In the vacuum-fired samples with $x < \frac{1}{3}$, the correlation of the peak position of band C with the lattice parameter (Fig. 6) indicates that each of these variables is proportional to a common factor that varies linearly with x. The most obvious common factor is the concentration of t_{2g} conduction electrons, which decreases linearly with increasing x.

From Vegard's law, and the smaller size of a Ti^{4+} ion relative to the Ti^{3+} ion, the lattice parameter is expected to decrease linearly with increasing x as observed (*15*). Thus an empirical connection between the concentration of t_{2g} conduction electrons and the lattice parameter is established.

Evidence for a parallel decrease in the width of the t_{2g} conduction band with increasing x comes from Fig. 4. Band B has been attributed to transitions between the oxygen-2p valence band and the t_{2g} conduction band. Ultraviolet PE spectra (*16*) have shown that the oxygen-2p band does not change significantly with composition, so the width of band B should reflect the width of the empty portion of the t_{2g} band. Since the fraction of t_{2g} states that are empty increases with x, the decrease in the width of band B in Fig. 4 clearly indicates a corresponding narrowing of the t_{2g} band with increasing x. Thus an empirical connection between the concentration of t_{2g} conduction electrons and the width of the t_{2g} band is established. An explanation of this relationship between the width of the t_{2g} band and the concentration of conduction electrons remains to be made.

In the tight-binding approximation (*20, 21*), the bandwidth for a periodic array of titanium atoms is proportional the mean number of nearest-neighbor titanium atoms, z, and to the overlap integral for t_{2g} orbitals on nearest-neighbor titanium atoms. Thus, it is not immediately obvious why the bandwidth is observed to decrease with the lattice parameter; the slow decrease in the value of z with increasing x cannot be invoked as the overlap integral increases sensitively with decreasing separation of the titanium atoms if the concentration of t_{2g} electrons is kept fixed. On the other hand, the concentration of t_{2g} electrons decreases with increasing x. Since the conduction electrons screen one another from the positive potential of the titanium ions, the radial extension of the t_{2g} wavefunctions decreases with increasing x. This process directly opposes the effect of changes in the lattice parameter on the overlap integral, and it would appear to be dominant. In addition, the lithium ions enter the octahedral sites randomly and destroy the translational symmetry of the

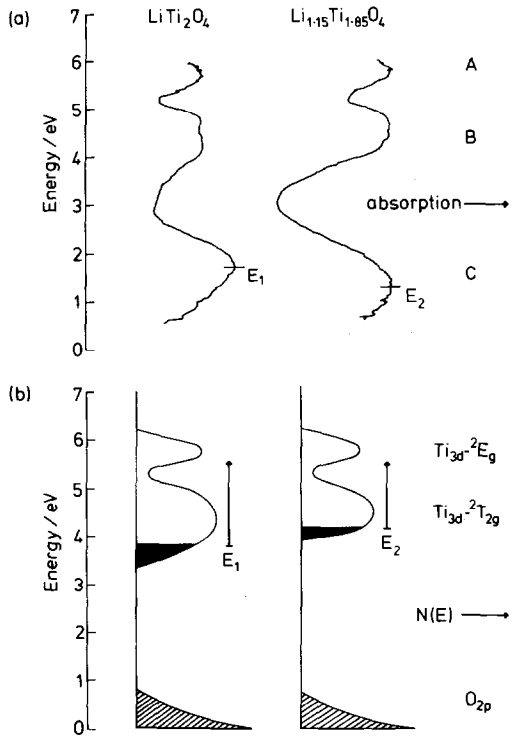

FIG. 8. (a) The room-temperature diffuse-reflectance spectra and (b) the band structures of $LiTi_2O_4$ ($x = 0$) and $Li_{1.15}Ti_{1.65}O_4$ ($x = 0.15$).

array of titanium atoms. Trapping of electrons in the localized states of a band tail can only further reduce any screening from the other t_{2g} conduction electrons.

If we now postulate that band C arises from electrons excited from the partially filled t_{2g} conduction band to states in the empty σ^* band, the peak corresponding to electrons excited from localized states at the bottom of the t_{2g} band, we can explain the compositional dependence of the peak energy of band C. This energy is indeed compatible with the separation of the t_{2g} and σ^* bands, and the variation in the peak energy of the band C with composition closely follows the variation in the width of the t_{2g} band with composition. This is shown schematically for two compositions, $x = 0$ and $x = 0.15$, in Fig. 8.

In the vacuum-fired samples with $x < \frac{1}{3}$, the t_{2g} conduction band narrows with increasing lithium content due to the decreasing efficiency of the screening by itinerant conduction electrons. The energies of the localized states at the bottom of the t_{2g} band, move with the band edge; therefore they increase in energy, and the peak position of band C decreases in energy with increasing lithium content. The peak intensity of band C follows the concentration of these localized states and decreases slowly with increasing lithium content.

In the hydrogen-reduced samples with $x = \frac{1}{3}$, the t_{2g} conduction band does not narrow with increasing degree of reduction because the electrons introduced are not itinerant conduction electrons and therefore do no screening. Consequently, the energies of the localized states at the bottom of the t_{2g} band do not change, and the peak position of band C does not change with increasing degree of reduction. However, this peak position contains the additional binding energy due to electrons trapping at hydroxyl ions or possibly oxygen vacancies. The peak intensity of band C follows the concentration of these localized states and increases with increasing degree of reduction.

Acknowledgments

We thank the SERC for financial support and Dr. R. G. Egdell for assistance with the diffuse-reflectance measurements.

References

1. A. DESCHANVRES, B. RAVEAU, AND Z. SEKKAL, *Mater. Res. Bull.* **6**, 699 (1971).
2. D. C. JOHNSTON, H. PRAKASH, W. H. ZACHARIASEN, AND R. VISWANATHAN, *Mater. Res. Bull.* **8**, 777 (1973).
3. D. C. JOHNSTON, Ph.D. thesis, University of California–San Diego (1975).
4. D. C. JOHNSTON, *J. Low-Temp. Phys.* **25**, 145 (1976).

5. R. W. McCallum, D. C. Johnston, C. A. Luengo, and M. B. Maple, *J. Low-Temp. Phys.* **25,** 177 (1976).
6. R. N. Shelton, D. C. Johnston, and H. Adrian, *Solid State Commun.* **20,** 1077 (1976).
7. S. Foner and E. J. McNiff, *Solid State Commun.* **20,** 995 (1976).
8. U. Roy, A. Das Gupta, and C. C. Koch, *IEEE Trans. Magn.* **MAG-13** 836 (1976).
9. U. Roy, K. Petrov, I. Tsolovski, and P. Peshev, *Phys. Status Solidi A* **44,** K25 (1977).
10. K. Petrov and I. Tsolovski, *Phys. Status Solidi A* **58,** K85 (1980).
11. A. H. Mousa and N. W. Grimes, *J. Mater. Sci.* **15,** 739 (1980).
12. T. Inukai, T. Murakami, and T. Inamura, *Jpn. J. Appl. Phys.* **20,** L264 (1980).
13. T. Inukai, T. Murakami, and T. Inamura, *Jpn. J. Appl. Phys.* **20,** L681 (1981).
14. M. R. Harrison, D.Phil. thesis, Oxford University (1981).
15. M. R. Harrison, P. P. Edwards, and J. B. Goodenough, *J. Solid State Chem.* **54,** 426 (1984).
16. P. P. Edwards, R. G. Egdell, I. Fragala, J. B. Goodenough, M. R. Harrison, A. F. Orchard, and E. G. Scott, *J. Solid State Chem.* **54,** 127 (1984).
17. J. B. Goodenough, *Prog. Solid State Chem.* **5,** 145 (1971).
18. N. F. Mott, "Metal-Insulator Transitions", Taylor & Francis, London (1974).
19. W. W. Wendlandt and H. G. Hecht, "Reflectance Spectroscopy," Interscience, New York (1966).
20. O. Madelung, "Introduction to Solid-State Theory," Springer-Verlag, Heidelberg (1978).
21. R. J. Elliott and A. F. Gibson, "An Introduction to Solid-State Physics and its Applications," MacMillan & Co., London (1974).
22. P. G. Dickens, R. M. P. Quilliam, and M. S. Whittingham, *Mater. Res. Bull.* **3,** 941 (1968).
23. J. F. Owen, K. J. Teegarden, and H. R. Shanks, *Phys. Rev. B* **18,** 3827 (1978).
24. R. E. Dietz, M. Campagna, J. N. Chazalviel, and H. R. Shanks, *Phys. Rev. B* **17,** 3790 (1978).
25. D. C. Cronemayer, *Phys. Rev.* **87,** 876 (1952).
26. O. W. Johnson, *Phys. Rev.* **136,** A-284 (1964).
27. O. W. Johnson, W. D. Ohlsen, and P. I. Kingsbury, *Phys. Rev.* **175,** 1102 (1968).
28. M. Guermazi, P. Thevenard, P. Faisant, M. G. Blanchin, and C. H. S. Dupuy, *Radiat. Eff.* **37,** 99 (1978).
29. M. Guermazi, P. Thevenard, M. Treilleux, and C. H. S. Dupuy, *Mater. Res. Bull.* **15,** 147 (1980).
30. V. N. Bogomolov, E. K. Kudinov, D. N. Mirlin, and Y. A. Firsov, *Sov. Phys. Solid State* **9,** 1630 (1968).
31. D. C. Cronemayer, *Phys. Rev.* **113,** 1222 (1959).
32. C. J. Ballhausen and H. B. Gray, *Inorg. Chem.* **1,** 111 (1962).
33. "International Tables for X-Ray Crystallography," Vol. I, Kynoch, Birmingham (1965).